

# Travelling wave protection with disturbance classification for distribution grids with distributed generation

**Conference Paper****Author(s):**

Davydova, Nadezhda; Hug, Gabriela

**Publication date:**

2018-10-25

**Permanent link:**

<https://doi.org/10.3929/ethz-b-000312963>

**Rights / license:**

[Creative Commons Attribution 3.0 Unported](#)

**Originally published in:**

The Journal of Engineering 2018(15), <https://doi.org/10.1049/joe.2018.0176>

# Travelling wave protection with disturbance classification for distribution grids with distributed generation

eISSN 2051-3305

Received on 3rd May 2018

Accepted on 23rd May 2018

E-First on 20th August 2018

doi: 10.1049/joe.2018.0176

www.ietdl.org

Nadezhda Davydova<sup>1</sup> ✉, Gabriela Hug<sup>1</sup><sup>1</sup>Power Systems Laboratory, ETH Zurich, Switzerland

✉ E-mail: davydovn@eeh.ee.ethz.ch

**Abstract:** The high penetration of distributed generation in distribution grids and the development of microgrids may cause the malfunctioning of the conventional distribution level protection systems. Despite multiple works dedicated to addressing this problem, the development of reliable, high-speed, and cost-efficient protection systems for active grids remains a topical issue. This study proposes a protection system for medium voltage lines that relies entirely on the analytical description of travelling wave transients. This protection uses only local high-frequency current measurements and power-frequency voltage measurements, which potentially makes it a low-cost yet reliable solution. The protection system operates securely by not tripping healthy lines in case of disturbances that do not lead to any faults. The proposed protection is tested on the IEEE 34-bus distribution system with distributed generation.

## 1 Introduction

With the high penetration of distributed generation (DG) and the development of microgrids in distribution systems, these systems acquire new properties: bidirectional power flows, decrease in short circuit (SC) current levels due to the deployment of converter-based DGs, and different SC levels in connected and islanded operations of microgrids. According to [1, 2], the conventional overcurrent protection systems, which are widely used on the distribution level, may fail to reliably protect these so-called active distribution grids.

To address the challenges of active grids, there have been considerable research efforts to develop protection systems adaptive to changes in active grids. Adaptive protection systems that rely only on local measurements can be found, for example, in [2, 3]. The utilisation of both voltage and current measurements makes these protection systems robust to changes in active grids. For the same reason, the conventional distance protection system, which is mainly used on the transmission level, can reliably protect active grids. However, these protection systems are non-unit systems [4], therefore, they act with time delays, which may not be acceptable in grids with DGs.

The problem of the fault clearing time can be effectively addressed by conventional differential or communication-assisted adaptive protections such as those proposed in [1, 5, 6]. These protection systems have better observability of the current state of a distribution grid than protection systems based on local measurements; therefore, they require less time for making reliable decisions. While communication-assisted protection systems can successfully protect active grids, the communication links that they rely on are costly and may cause reliability issues in case of the loss of connections.

An alternative way to address challenges imposed by active grids is to develop protection systems based on the travelling wave (TW) theory. Fault-generated TWs that are analysed in the TW protection systems are essentially not affected by the operation modes of DGs and microgrids, which make these protection systems a viable solution for active grids. In addition, the fault clearing time of the TW-based protection systems can be potentially small enough to enable the stable operation of the DGs in the presence of faults in active grids since wave transients are fast developing phenomena. TW-based protections for distribution grids with DGs can be found, for instance, in [7–10]. While protection systems in [7, 8] can work effectively in active grids, they rely on a communication infrastructure and thus are costly and

may malfunction in case of the loss of communication links. The protection system in [9] relies on local current and voltage measurements for detecting single-phase-to-ground faults on power lines. However, it may have problems related to the poor transfer characteristics of conventional voltage transformers and close-in faults. In [10], we propose a protection system that requires only local high-frequency current measurements to protect medium voltage lines against all types of faults. The protection algorithm consists of two main steps: direction detection and fault location (FL). Initially, the direction detection algorithm identifies the fault direction with respect to the protection terminal's location using the analytical description of TW transients. Then the FL algorithm classifies a detected fault as internal or external utilising neural networks (NNs). Although this protection system was shown to operate satisfactorily in active grids, it has some intrinsic problems. Since the NNs are data-driven methods, the FL algorithm potentially cannot provide sufficient reliability in real power systems, where the number of potential system states is innumerable. Moreover, this algorithm relies on the assumption that angles between a bus voltage at the terminal's location and currents through protected lines are constant which may be unrealistic. In addition, while the protection system was shown to operate securely in case of switching transients, it may malfunction in case of disturbances that do not cause faults but generate fault-like TWs.

This study presents a TW protection system for medium voltage lines in active grids that builds on the protection system proposed in [10] but aims to address its aforementioned shortcomings. The protection system uses local high-frequency current measurements and power-frequency voltage measurements, which potentially makes it a low-cost solution because it requires neither communication links nor voltage transformers capable of capturing high-frequency TWs. The utilisation of both voltage and current measurements enables removing the assumption with regard to angles between voltage and currents that the algorithm in [10] relies on.

The main contribution of this work is two-fold. First, the FL algorithm based on the analytical description of the TW transients and the analysis of their energy is developed. The advantage of this algorithm is that it is based on physical considerations as opposed to the data-driven machine learning algorithm used in [10]. Second, the disturbance classification (DC) algorithm is derived to increase the security of the protection system in case of the occurrence of

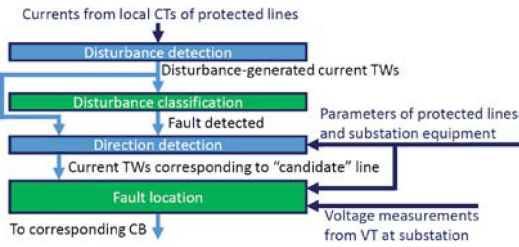


Fig. 1 Proposed protection algorithm

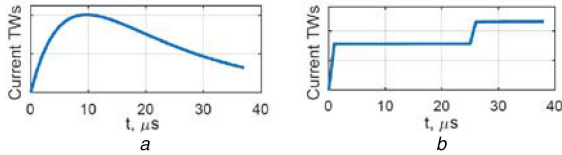


Fig. 2 Typical waveforms of current TWs  
(a) Lightning-generated, (b) Fault-generated

the lightning strokes without flashover that do not lead to faults but generates fault-like TWs.

## 2 Proposed protection system

### 2.1 Algorithm overview

The proposed protection algorithm shown in Fig. 1 is intended for implementation in microprocessor terminals installed at each substation of the active distribution grids. Each of the terminals performs simultaneous protection of all medium voltage lines interconnected at a given substation. The protection algorithm requires local measurements from current transformers (CTs) of the protected lines and a voltage transformer (VT) at the substation. The protected lines are assumed to have circuit breakers (CBs) at both ends to improve fault localisation.

The protection algorithm consists of four main blocks: disturbance detection, DC, direction detection, and FL. Initially, the disturbance detection block analyses three-phase currents from all protected lines by the means of modal transformation and discrete wavelet transform to detect TWs generated by a disturbance in the vicinity of a protection terminal. If the disturbance is detected, disturbance-generated TWs are extracted from the input currents. The detailed description of the disturbance detection algorithm is presented in [10]. The disturbance-generated TWs are then used by the DC block to identify whether the disturbance is a fault or a lightning stroke without flashover. In case the disturbance is classified as a fault, the protection algorithm triggers the direction detection block that utilises the current TWs from all protected lines to determine a particular protected line ('candidate' line) in the direction of which the fault has occurred. The fault direction is obtained by constructing the TWs' equations for various fault directions and testing their validity with the input data. The detailed description of the direction detection algorithm is also presented in [10]. After the 'candidate' line is identified, the FL block determines whether the fault is internal or external. In case of the internal fault, the protection terminal sends a tripping signal to the local CB of the faulted line.

In the following, we describe the new DC and FL blocks. As mentioned, the other blocks are equivalent to our previous work and the reader is referred to [10] for details on these blocks.

### 2.2 Disturbance classification

The DC block aims to identify whether the disturbance detected by the disturbance detection block is a fault or a lightning stroke to a phase wire without flashover. The main idea behind the DC algorithm is that the waveforms of the current TWs generated by a fault and lightning are different. Fig. 2 shows the typical waveforms of the current TWs launched by a fault and lightning without flashover. The surge-like waveform of the lightning-generated current TWs can be expressed analytically as follows:

$$i = I \cdot (\exp(-a \cdot t)) - (\exp(-b \cdot t)), \quad (1)$$

where  $t$  is the time coordinate,  $I$ ,  $a$ , and  $b$  are constant coefficients. According to [11, 12], for typical lightning waveforms, the values of  $I$ ,  $a$  and  $b$  are of order  $10^1$  kA,  $10^4$  s $^{-1}$  and  $10^6$  s $^{-1}$ , respectively. For these values of the coefficients, the absolute value of the time derivative taken at the tail of the lightning waveform is of order  $10^1$  A/ $\mu$ s. Since a fault generates step-like current TWs, the absolute value of the derivative taken at the tail of these TWs is much less than  $10^1$  A/ $\mu$ s. Therefore, the DC algorithm is based on the comparison of the absolute value of the time derivative taken at the tail of the disturbance-generated current TWs with the predefined threshold  $L_{set}$ . If the absolute value of the derivative is less than  $L_{set}$ , then the disturbance is classified as a fault. Otherwise, it is considered to be a lightning stroke without flashover. It is important to mention that before calculating the derivative, the DC algorithm performs pre-processing of the input current TWs to improve the classification accuracy. Initially, the input three-phase current TWs corresponding to all protected lines are transformed into modal components since the simulation results showed that the DC algorithm had higher classification accuracy when it was based on the modal rather than phase quantities. Among all the obtained modal currents, the one with the highest transient energy level [13] in a range of frequencies typical for faults and lightning [12] is chosen for the further analysis as it contains more information about the disturbance than other currents. Next, the DC algorithm performs fitting of (1) to the chosen modal current TWs to identify the general trend of the TWs' waveform thus reducing the impact of noise. Function (1) is chosen for fitting since it is a continuous differentiable function that can successfully capture a general trend of both lightning and fault-generated waveforms. The obtained fitting function is then used for the derivative calculation.

### 2.3 Fault location

The FL block is intended for identification whether the fault has occurred on the 'candidate' line or it is an external fault. This block receives three-phase fault-generated current TWs corresponding to the local CTs of the 'candidate' line and the power-frequency voltage measurements from the VT at the considered substation. To identify whether the 'candidate' line is faulted, the energy of the input current TWs is compared with a threshold value  $E_{set}$ , which depends on the type and inception angle of a fault. The idea behind the comparison is that the energy of fault-generated TWs obtained around the protection terminal decreases as a FL is further away from the terminal. Therefore, if the energy is greater than the threshold, the fault is internal and the corresponding local circuit breaker is tripped. The value of the inception angle is obtained from voltage measurements. The type of fault is identified by analysing equations that describe the behaviour of the TWs launched by the different types of faults and selecting the one that matches the input data from the 'candidate' line the best.

The FL algorithm, therefore, consists of three successive steps: fault inception angle identification, fault type detection, and analysis of TWs' energy.

**2.3.1 Fault inception angle identification:** In this study, the fault inception angle is defined as the phase-A voltage angle at the FL and at the moment of fault initiation. Due to the small angle difference between voltages at two ends of a distribution line and the high speed of TWs' propagation, the fault inception angle is assumed to be identical to the phase-A voltage angle at the considered substation at the moment of the arrival of the fault-generated TWs at the substation. Therefore, the fault inception angle is determined using the input phase-A voltage measurements and the TWs arrival moment identified by the disturbance detection algorithm. According to Fig. 3, the inception angle  $\alpha$  can be calculated as follows:

$$\alpha = \begin{cases} t \cdot 360^\circ & \text{if } V > 0, \\ 180^\circ & \text{if } V = 0 \& V' > 0, \\ 0^\circ & \text{if } V = 0 \& V' < 0, \\ 180^\circ + t \cdot 360^\circ / T & \text{if } V < 0, \end{cases} \quad (2)$$

where  $T$  is the power-frequency period,  $t$  is the time period between the last phase-A voltage zero crossing and the TWs arrival moment,  $V$  and  $V'$  are the voltage measurements at the TWs arrival moment and one discretisation step  $\Delta t$  earlier, respectively. Compared to the inception angle detection algorithm presented in [10], this algorithm works for any value of the angle between a voltage at the terminal's location and a current through the 'candidate' line.

**2.3.2 Fault type detection:** After the inception angle is identified, the FL algorithm detects the type of the fault among all possible types, except for complex types where several faults occur simultaneously in different parts of the grid. To illustrate the idea behind the fault type detection algorithm, let us consider a part of the distribution grid with substations  $M$  and  $N$  interconnected by line  $L1$  shown in Fig. 4. Substation  $M$  has  $m$  lines and a transformer  $T1$ . A similar set of power equipment is installed at substation  $N$ . Assume that the fault  $F$  has occurred on  $L1$  at the moment when phase voltages  $V_f$  at the FL were equal to

$$\begin{aligned} V_{af} &= V_m \cdot \sin(\alpha), \\ V_{bf} &= V_m \cdot \sin(\alpha - 120^\circ), \\ V_{cf} &= V_m \cdot \sin(\alpha + 120^\circ), \end{aligned} \quad (3)$$

where  $V_m$  is the amplitude of the pre-fault voltages. This fault can be modelled as a superposition of two sets of phase voltages at the FL: pre-fault voltages  $V_{af}$ ,  $V_{bf}$ ,  $V_{cf}$  and step-like cancellation voltages  $e_{af}$ ,  $e_{bf}$ ,  $e_{cf}$  [12]. The cancellation voltages are determined by the fault type and pre-fault voltages. The cancellation voltages initiate the propagation of voltage and current TWs through the grid according to the telegraph equations [12]. Since, in phase quantities, all these voltages and currents are coupled, appropriate linear modal transformations can be used for decoupling them and thus facilitating the analysis of wave transients. Modal cancellation voltages are given by

$$\begin{bmatrix} e_{af}^\alpha \\ e_{bf}^\beta \\ e_{cf}^0 \end{bmatrix}^T = \mathbf{A} \begin{bmatrix} e_{af} \\ e_{bf} \\ e_{cf} \end{bmatrix}^T, \quad (4)$$

where  $\mathbf{A}$  is the modal transformation matrix. In this study, it is assumed that the protected grid is balanced; therefore, the Clarke matrix is used as  $\mathbf{A}$ . In this case,  $e_f^\alpha$  and  $e_f^\beta$  are the  $\alpha$  and  $\beta$  line modes and  $e_f^0$  is the ground mode. These modal components can also be expressed as follows:

$$\begin{aligned} e_f^\alpha &= f_\alpha(V_{af}, V_{bf}, V_{cf}), \\ e_f^\beta &= f_\beta(V_{af}, V_{bf}, V_{cf}), \\ e_f^0 &= f_0(V_{af}, V_{bf}, V_{cf}). \end{aligned} \quad (5)$$

where  $f_\alpha$ ,  $f_\beta$ , and  $f_0$  are the functions that are determined by a fault type and provided in [14]. It is important to note that a non-zero ground mode of voltage and current TWs indicates that a ground fault has occurred in the grid; otherwise, the TWs are generated by a fault without ground.

Since different modes are independent of each other, a single-mode circuit can be constructed to analyse the behaviour of fault-generated modal TWs at particular time and space coordinates. Fig. 5a shows an  $\alpha$ -mode circuit for analysis of the TWs around the FL immediately after the fault inception. As can be seen from the figure, incident voltage TWs  $e_{in}^{\alpha l}$  and  $e_{in}^{\alpha r}$  that propagate to the left and right from the FL are identical to  $e_f^\alpha$ . Analogously, incident

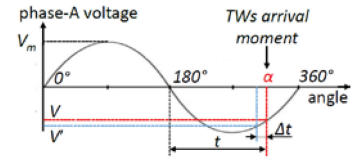


Fig. 3 Fault inception angle identification

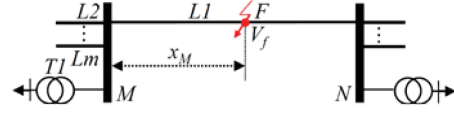


Fig. 4 Considered part of distribution grid

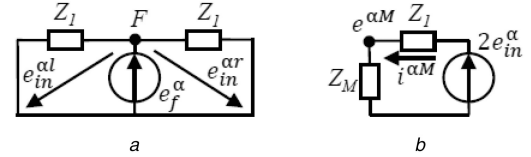


Fig. 5  $\alpha$ -Mode circuits for analysis of TWs at different locations (a) FL, (b) Substation  $M$

voltage TWs corresponding to  $\beta$  and zero modes are identical to  $e_f^\beta$  and  $e_f^0$ , respectively. Therefore, the following equation holds:

$$\begin{bmatrix} e_{in}^{\alpha l} \\ e_{in}^{\beta l} \\ e_{in}^{0l} \end{bmatrix} = \begin{bmatrix} e_{in}^{\alpha r} \\ e_{in}^{\beta r} \\ e_{in}^{0r} \end{bmatrix} = \begin{bmatrix} e_f^\alpha \\ e_f^\beta \\ e_f^0 \end{bmatrix}. \quad (6)$$

Fault-generated TWs  $e_{in}^{\alpha l}$ ,  $e_{in}^{\beta l}$ ,  $e_{in}^{0l}$  and  $e_{in}^{\alpha r}$ ,  $e_{in}^{\beta r}$ ,  $e_{in}^{0r}$  undergo attenuation and dispersion, while propagating towards substations  $M$  and  $N$ , respectively. Without loss of generality, let us consider the behaviour of the TWs around  $M$ . According to the TW theory, the incident voltage TWs that arrive at  $M$  are given by [12]

$$\begin{aligned} e_{in}^{\alpha M} &= e_{in}^{\alpha l} \cdot \exp(-\gamma \cdot x_M), \\ e_{in}^{\beta M} &= e_{in}^{\beta l} \cdot \exp(-\gamma \cdot x_M), \\ e_{in}^{0M} &= e_{in}^{0l} \cdot \exp(-\gamma_0 \cdot x_M), \end{aligned} \quad (7)$$

where  $x_M$  is the distance from the FL to  $M$ ,  $\gamma$  and  $\gamma_0$  are the line and ground mode propagation constants, respectively. Since substation  $M$  can be considered as a symmetrical discontinuity point, the incident TWs interact with it by generating reflected  $e_r^{\alpha M}$ ,  $e_r^{\beta M}$ ,  $e_r^{0M}$  and transmitted  $e_t^{\alpha M}$ ,  $e_t^{\beta M}$ ,  $e_t^{0M}$  voltage TWs that are given by [12]

$$\begin{aligned} e_r^{\alpha M} &= (Z_M - Z_1) \cdot e_{in}^{\alpha M} / (Z_M + Z_1), \\ e_r^{\beta M} &= (Z_M - Z_1) \cdot e_{in}^{\beta M} / (Z_M + Z_1), \\ e_r^{0M} &= (Z_{M0} - Z_0) \cdot e_{in}^{0M} / (Z_{M0} + Z_0), \\ e_t^{\alpha M} &= 2Z_M \cdot e_{in}^{\alpha M} / (Z_M + Z_1), \\ e_t^{\beta M} &= 2Z_M \cdot e_{in}^{\beta M} / (Z_M + Z_1), \\ e_t^{0M} &= 2Z_{M0} \cdot e_{in}^{0M} / (Z_{M0} + Z_0), \end{aligned} \quad (8)$$

where  $Z_1$  and  $Z_0$  are the surge impedances of  $L1$  corresponding to the line and ground modes,  $Z_M$  and  $Z_{M0}$  are the equivalent impedances of substation  $M$  corresponding to the line and ground modes. Considering (6)–(8) together, we can conclude that while TWs induced by the cancellation voltages undergo significant changes when propagating through the grid, the ratio between the line modes of cancellation voltages  $e_f^\alpha/e_f^\beta$  is preserved in incident voltage TWs and TWs reflected and transmitted at substations.

The reflected TWs  $e_r^{\alpha M}$ ,  $e_r^{\beta M}$ ,  $e_r^{0M}$  then propagate from  $M$  towards the FL where they undergo reflection and transmission. Since, in the general case, the FL can be considered as an asymmetric discontinuity point, it couples different modal components.

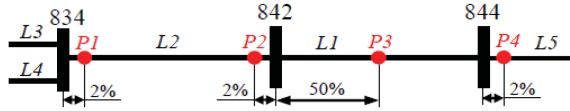


Fig. 6 Part of IEEE 34-bus distribution grid

According to the TW theory, the reflected  $e_r^{\alpha F}$ ,  $e_r^{\beta F}$ ,  $e_r^{0F}$  and transmitted  $e_t^{\alpha F}$ ,  $e_t^{\beta F}$ ,  $e_t^{0F}$  TWs at the FL are given by

$$\begin{aligned} e_r^{\alpha F} &= f_\alpha(e_r^{\alpha M}, e_r^{\beta M}, e_r^{0M}), \\ e_r^{\beta F} &= f_\beta(e_r^{\alpha M}, e_r^{\beta M}, e_r^{0M}), \\ e_r^{0F} &= f_0(e_r^{\alpha M}, e_r^{\beta M}, e_r^{0M}), \\ e_t^{\alpha F} &= e_r^{\alpha M} \cdot \exp(-\gamma \cdot x_m) + e_r^{\alpha F}, \\ e_t^{\beta F} &= e_r^{\beta M} \cdot \exp(-\gamma \cdot x_m) + e_r^{\beta F}, \\ e_t^{0F} &= e_r^{0M} \cdot \exp(-\gamma_0 \cdot x_m) + e_r^{0F}. \end{aligned} \quad (9)$$

Despite the fact that these TWs depend on a mixture of modal components of  $e_r^M$ , it can be shown that the ratio between the line modes of cancellation voltages is still preserved in these TWs.

From the presented analysis, we can conclude that the ratio between the line modes of the cancellation voltages is characterised by two properties: it is determined by the fault type and it is constant at any point in the grid and any moment after the fault initiation. Therefore, the ratio can be considered as a suitable criterion for the fault type detection in the protection terminals.

Assume that a protection terminal with the proposed protection algorithm is installed at substation  $M$ . Since the algorithm obtains only local current TWs and not voltage TWs, let us derive the ratio  $e^{\alpha M}/e^{\beta M}$  between the line modes of voltage TWs at substation  $M$  as a function of the obtained current TWs. Fig. 5b shows an  $a$ -mode circuit for analysis of the  $a$ -mode TWs around substation  $M$  after the fault inception. Here,  $i^{\alpha M}$  is the total current TW that in general contains multiple reflections from both substation equipment and the FL,  $e_m^\alpha$  is the incident voltage TW. The  $a$ -mode voltage TW at  $M$  is given by

$$e^{\alpha M} = i^{\alpha M} \cdot Z_M. \quad (10)$$

A similar expression can be obtained for  $e^{\beta M}$  as a function of  $\beta$ -mode total current TW  $i^{\beta M}$ . The ratio between  $\alpha$  and  $\beta$  line modes of voltage TWs at substation  $M$  is as follows:

$$e^{\alpha M}/e^{\beta M} = i^{\alpha M}/i^{\beta M}. \quad (11)$$

Based on all of the analysis presented above, the following fault-type identification algorithm is proposed. Initially, the input current TWs corresponding to the ‘candidate’ line are transformed into modal components  $i^{\alpha M}$ ,  $i^{\beta M}$ , and  $i^{0M}$ . Next, the fault is classified as a fault with or without ground by comparing ground component  $i^{0M}$  with the preset threshold  $i_{set}^0$ . If  $i^{0M}$  is greater than the threshold, the fault is considered to be a ground fault. Otherwise, a fault without ground is detected. After that, the pre-fault voltages  $V_f$  are calculated according to (3) using the obtained inception angle and the value of  $V_m$  measured by the VT at the substation. These voltages are then utilised with (5) to determine the ratios between the line modes of cancellation voltages for all types of faults corresponding to the identified class. Next, the ratio between the line modes  $i^{\alpha M}/i^{\beta M}$  is calculated and subtracted from the obtained ratios for the cancellation voltages. According to (11), the type of fault that gives the smallest absolute value of the difference is considered to be the output of the fault-type detection algorithm.

**2.3.3 Analysis of current TWs energy:** Based on the inception angle and fault type obtained on the previous steps of the FL algorithm, the threshold value  $E_{set}$  is determined from a look-up table. This table is constructed experimentally to distinguish

furthest internal and closest external faults. Next, the energy of the three-phase current TWs corresponding to the ‘candidate’ line is calculated as follows:

$$E = \sum_{k=1}^d \left( (i^{\alpha M}(k))^2 + (i^{\beta M}(k))^2 + (i^{0M}(k))^2 \right), \quad (12)$$

where  $i^{\alpha M}$ ,  $i^{\beta M}$  and  $i^{0M}$  are phase current TWs,  $k$  is the sampling index,  $d$  is the total number of considered samplings. The obtained energy  $E$  is compared with the threshold  $E_{set}$ . If  $E$  is greater than  $E_{set}$ , the ‘candidate’ line is faulted and the corresponding CB is tripped. Otherwise, the ‘candidate’ line is healthy.

### 3 Simulation results

This section presents the results of testing the proposed protection system on the IEEE 34-bus distribution system with different types of DGs. First, the experimental setup is discussed followed by the testing of the developed DC and FL blocks of the protection system.

#### 3.1 Experimental setup

To evaluate the performance of the protection system in an active distribution grid, the IEEE 34-bus test system proposed in [15] was extended by connecting two wind generators to buses 848 and 832. Each wind generator was modelled as either an asynchronous generator or a full conversion type 4 wind farm (WF), thus making a total of four DG's composition scenarios. Standard models provided in EMTP-RV were utilised for both generator types. Under-voltage protection was implemented in the DGs with time voltage characteristics set according to the German Grid Code [16]. The length of lines in the test system was chosen to be 5 km. The nominal grid frequency was 50 Hz.

EMTP-RV software was used to perform simulations. The current measurements in the protection algorithm were sampled with 1 MHz frequency and stored for a 1 ms moving window. The voltage measurements were sampled with 2 kHz frequency and stored for a 11 ms moving window. The protection terminals were installed at buses 834, 842, and 844 in a part of the distribution grid shown in Fig. 6. To test their joint operation, a number of incidents were simulated in the grid such as different types of faults and lightning surges occurring at various locations and moments in time. The range of considered inception angles was from  $2^\circ$  to  $178^\circ$  and from  $182^\circ$  to  $358^\circ$  varying with a step of  $2^\circ$ . The line faults and lightning surges were simulated for the following locations in the percentage of line lengths: from 2 to 98% with a step of 6%. The lightning was modelled as a surge current source based on (1) with the following values of constant parameters:  $I = 33$  kA,  $a = 1.4 \times 10^4$  s $^{-1}$ , and  $b = 4.9 \times 10^6$  s $^{-1}$  [11].

#### 3.2 DC algorithm testing

This section presents the simulation results obtained for the DC blocks of the considered protection terminals. For each terminal, the value of threshold  $L_{set}$  in the DC block was chosen experimentally to be 10 A/ $\mu$ s. The Clarke transformation was used in all terminals for pre-processing of the input current TWs. The operation of the DC blocks of the protection terminals was tested for various fault and lightning instances and four DG's composition scenarios. Table 1 presents part of the results obtained by the DC block of the protection terminal at bus 842 for disturbances with  $2^\circ$  inception angle occurring at locations P1–P4 as shown in Fig. 6. The DG composition scenario is as follows: a full-conversion WF is on bus 848 and an asynchronous generator is on bus 832. As can be seen from the table, the absolute values of the derivatives calculated by the DC block are less than  $L_{set}$  for all considered fault instances and greater than  $L_{set}$  for lightning strokes. Similar results were obtained for other protection terminals, DG composition scenarios, and fault and lightning instances. Therefore, we can conclude that the criterion used in the DC algorithm allowed

**Table 1** Absolute values of derivative obtained by DC block of protection terminal at 842

Disturbance types		Locations			
		P1	P2	P3	P4
faults	ABC	0.027	0.023	0.019	0.020
	AB	0.014	0.018	0.004	0.003
	BCg	0.009	0.038	0.003	0.005
	Cg	0.002	0.084	0.000	0.041
lightnings	A	78.689	68.271	78.788	84.015
	B	35.105	34.131	38.443	42.003
	C	39.345	34.131	39.281	31.858

**Table 2** Absolute values of differences obtained by FL block of protection terminal at 842

Fault types	$\alpha = 2^\circ$				$\alpha = 90^\circ$			
	ABC	AB	BCg	Cg	ABC	AB	BCg	Cg
$\delta_{ABC}$	<b>2.9</b>	85.3	—	—	<b>3.1</b>	78.2	—	—
$\delta_{AB}$	86.7	<b>3.1</b>	—	—	67.2	<b>2.5</b>	—	—
$\delta_{BC}$	6.6	100	—	—	16.4	100	—	—
$\delta_{AC}$	100	18.5	—	—	100	16.4	—	—
$\delta_{ABg}$	—	—	6.4	10.9	—	—	89.9	1.7
$\delta_{BCg}$	—	—	<b>0.6</b>	100	—	—	<b>14.2</b>	8.1
$\delta_{ACg}$	—	—	100	1.1	—	—	100	100
$\delta_{Ag}$	—	—	6.9	6.8	—	—	93.3	1.1
$\delta_{Bg}$	—	—	5.9	13.6	—	—	87.5	2.3
$\delta_{Cg}$	—	—	8.0	<b>0.0</b>	—	—	99.1	<b>0.0</b>

successful classification of faults against lightning strokes without flashover.

### 3.3 FL algorithm testing

This section presents the results of testing the FL blocks of the considered protection terminals and the whole protection system for various fault instances and DG's composition scenarios. First, the performance of each step of the FL algorithm is assessed followed by the evaluation of the whole protection system.

The first step in the FL block is the fault inception angle identification algorithm. Over all simulated scenarios, the maximum error made by the algorithm in estimating the inception angle was  $0.0036^\circ$ . This error was sufficiently small to allow reliable operation of the successive steps of the FL algorithm.

The next step is the fault-type detection algorithm. For each protection terminal, the value of threshold  $I_{set}^o$  in this algorithm was chosen experimentally to be 0.1 A. Table 2 presents part of the results obtained by the fault type detection algorithm of the protection terminal at bus 842 for faults occurring at P2. The DG composition scenario was the same as in Table 1. Each column of Table 2 corresponds to one simulated fault instance. Each entry in the table is the absolute value of the difference  $\delta$  between the ratios of line modes of measured currents and cancellation voltages obtained with (5) for a particular type of fault. The differences in each column are given in percentage of the maximum difference in that column. Symbol '—' in some entries indicates that the fault type detection algorithm did not require these differences for fault type identification since comparison of the ground component of the input current with  $I_{set}^o$  excluded corresponding fault types from consideration. As can be seen from the table, the smallest entry at each column corresponds to the actually simulated fault type. Similar results were obtained for other protection terminals, DG composition scenarios, and fault instances. Therefore, we can conclude that the criterion used in the fault type detection algorithm allowed reliable identification of a fault type.

The last step of the FL algorithm is the comparison of the energy of the input current TWs corresponding to the 'candidate' line with the threshold  $E_{set}$ . For a particular fault type and inception angle, the value of  $E_{set}$  was chosen experimentally to distinguish furthest internal and closest external faults with the energies of input TWs  $E_{in}$  and  $E_{ex}$ , respectively. These faults were located 50

m from the remote end of the 'candidate' line. The results of testing this step of the FL algorithm in the considered protection terminals for various fault instances and DG's composition scenarios indicated that  $E_{set}$  chosen as  $(E_{in} + E_{ex})/2$  provided a reliable classification of internal and external faults.

The joint operation of the considered protection terminals was extensively tested for various fault and lightning instances and types of DGs. The simulation results showed that the proposed protection system operated reliably in active grids in case of lightning surges and different types of faults including close-in faults and faults with small inception angles. The protection system performed tripping of faulted lines in a time less than the time delay of the under-voltage protection of DGs thus enabling stable operation of DGs in active grids. This is an advantage of the proposed protection system over widely used conventional non-unit protections that in case of close-in faults have time delays greater than the delay of the under voltage protection.

## 4 Conclusion

This study presents a TW-based protection system for lines in active distribution grids that builds on the protection system proposed in [10] but aims to address its shortcomings. It requires only local high-frequency current measurements and power frequency voltage measurements, which potentially makes it a low-cost yet reliable solution. The main contribution of this work is two-fold. First, the FL algorithm that relies entirely on the analytical description of TW transients is developed. The advantage of this algorithm over the one proposed in [10] is that it is based on physical considerations as opposed to relying on data-driven approaches. Second, the DC algorithm is developed to enable secure operation of the protection system in case of lightning strokes without flashover. The simulation results demonstrate that the proposed protection system can operate reliably and with the required speed in grids with different types of DGs for various fault and lightning instances.

## 5 References

- [1] Coffele, F., Booth, C., Dysko, A.: 'An adaptive overcurrent protection scheme for distribution networks', *IEEE Trans. Power Deliv.*, 2015, **30**, (2), pp. 561–568

- [2] Mahat, P., Chen, Z., Bak-Jensen, B., *et al.*: 'A simple adaptive overcurrent protection of distribution systems with distributed generation', *Trans. Smart Grid*, 2011, **2**, (3), pp. 428–437
- [3] Liu, C., Chen, Z., Liu, Z.: 'A communication-less overcurrent protection for distribution system with distributed generation integrated'. IEEE Int. Symp. on Power Electronics for Distributed Generation Systems, Aalborg, Denmark, 2012, pp. 140–147
- [4] Makwana, V.H., Bhalja, B.R.: '*Transmission line protection using digital technology*' (Springer, Singapore, 2016)
- [5] Nailly, N.E., Saad, S.M., Elhaffar, A., *et al.*: 'Mitigating the impact of distributed generator on medium distribution network by adaptive protection scheme'. Eighth Int. Renewable Energy Congress, Amman, Jordan, 2017
- [6] Ma, J., Ma, W., Wang, X., *et al.*: 'A new adaptive voltage protection scheme for distribution network with distributed generations', *Can. J. Electric. Comput. Eng.*, 2013, **36**, (4), pp. 142–151
- [7] Li, X., Dysko, A., Burt, G.: 'Traveling wave-based protection scheme for inverter-dominated microgrid using mathematical morphology', *IEEE Trans. Smart Grid*, 2014, **5**, (5), pp. 2211–2218
- [8] Perera, N., Rajapakse, A.D.: 'Agent-based protection scheme for distribution networks with distributed generators'. Power Engineering Society General Meeting, Montreal, Canada, 2006
- [9] Dong, X., Wang, J., Shi, S., *et al.*: 'Traveling wave based single-phase-to-ground protection method for power distribution system', *CSEE J. Power Energy Syst.*, 2015, **1**, (2), pp. 75–82
- [10] Davydova, N., Hug, G.: 'Traveling wave based protection for medium voltage grids with distributed generation'. IEEE PowerTech, Manchester, 2017, pp. 1–6
- [11] Agrawal, S., Nigam, M.K.: 'Lightning phenomena and its effect on transmission line', *Rec. Res. Sci. Technol.*, 2014, **5**, pp. 183–187
- [12] Bewley, L.V.: '*Traveling waves on transmission systems*' (Wiley, New York, 1951)
- [13] Sharafi, A., Sanaye-Pasand, M., Jafarian, P.: 'Noncommunication protection of parallel transmission lines using breakers open-switching travelling waves', *IET Gen. Transm. Distrib.*, 2012, **6**, (1), p. 88
- [14] Phadke, A.G., Thorp, J.S.: '*Computer relaying for power systems*' (John Wiley & Sons Ltd, Oxford, UK, 2009)
- [15] Borghetti, A., Bosetti, M., Silvestro, M.D., *et al.*: 'Continuous-wavelet transform for fault location in distribution power networks: definition of mother wavelets inferred from fault originated transients', *IEEE Trans. Power Syst.*, 2008, **23**, (2), pp. 380–388
- [16] Benbouzid, M., Beltran, B., Amirat, Y., *et al.*: 'Second-order sliding mode control for DFIG-based wind turbines fault ride through capability enhancement', *ISA Trans.*, 2014, **53**, (3), pp. 827–833